Al-Qadisiyah JournalFor Engineering Sciences 18 (2025) 465 – 474

Contents lists available at: http://qu.edu.iq

Al-Qadisiyah Journal for Engineering Sciences

Journal homepage: https://qjes.qu.edu.iq

Research Paper

Combined bending and torsion behavior of externally strengthened RC beams via enlargement section and hybrid reinforcement

Abrar R. Al-Rammahi [1,2], ***Alaa M. Al-Khekany*** [1]✉, ***and György L. Balázs*** [3]

[1]*Department of Civil Engineering, College of Engineering, University of Al-Qadisiyah, Qadisiyah, Iraq.*
[2]*Ministry of Education, General Directorate of Education of Qadisiyah, Qadisiyah, Iraq.*
[3]*Department of Construction Materials and Technologies, Faculty of Civil Engineering, Budapest University of Technology and Economics, Budapest, Hungary.*

ARTICLE INFO

Article history:
Received 26 March 2024
Received in revised form 10 April 2025
Accepted 20 October 2025

keyword:
Concrete jacket
GFRP bar
Hybrid reinforcement
Section enlargement
Torsional strength

ABSTRACT

Despite extensive studies on reinforced concrete beams with fiber-reinforced polymer sheets, uncertainties persist regarding their behavior under complex torsional bending loads. This study investigated the combined bending and torsional behavior of RC beams externally reinforced by hybrid expansion and reinforcement sections. In this research, nine beams were cast using normal-strength reinforced concrete (NSC), with cross-sectional dimensions of 150 x 250 *mm*, and a total length of 1750 *mm*. One beam was left untouched to serve as a control specimen, and eight of them were reinforced using a sectional expansion technique using self-consolidating concrete (SCC) reinforced with steel, glass fiber reinforced polymer (GFRP) or hybrid reinforce (steel and GFRP). The eight samples were classified into two groups. The first group included 4 samples with a magnification section of 50 *mm* (Δh = 50 *mm*) and the second group included 4 samples with a magnification section of 75 *mm* (Δh = 75 *mm*). Nine beams were subjected to combined torsional bending loads, and tests focused on the effect of raising the Δh value, which increases the effective depth, and the GFRP replacement ratio (0% to 100%). Finally, the two groups' samples were compared for ultimate torsional strength, torsional moment, bending moment, and maximum torsion angle. Expanding the section (Δh = 50) resulted in a 33.33% to 66.67% increase in bending and torsion resistance compared to the control sample. For specimens with an expanded section (Δh = 75), the combined torsional and bending strength increased from 60% to 100%. Due to GFRP's brittleness, increasing the replacement ratio decreases the specimens' capacity to resist combined bending and torsion.

1. Introduction

In addition to bending and shear forces, reinforced concrete (RC) structural elements such as spiral staircases, ring beams at the bottom of circular tanks, end beams of shell roofs, beams supporting canopy panels, and end beams on each floor of multi-story buildings are subjected to significant torsional loading [1]. Torsional moments provide shear stresses by twisting structural elements longitudinally. Torsion usually occurs in conjunction with bending moment and shear stress, so structural elements are rarely subjected to torsional moment alone [2]. Torsional moments occur in a large number of structural members, including bridges, so torsional strengthening of concrete members for the purpose of bearing torsional stresses can be achieved in one of the following ways: (a) increasing the cross-sectional area of members; (b) adding transverse reinforcement (c) utilizing steel plates that are externally bonded, and (d) using external prestressing to apply an axial load to the member. Corrosion of steel reinforcement in concrete structures is a major constraint for the construction sector [3]. Given the issues of durability and corrosion faced by steel reinforcement in harsh environments, other materials such as fiber reinforcement polymers (FRP) have emerged as potential substitutes for reinforcement. Reinforcing bars are composite materials consisting of reinforcing fibers and a resin matrix. FRP composites are utilized in various engineering structures to improve performance requirements, thanks to their favorable features. FRP composites are used in the fields of rehabilitation, formwork, and reinforcement for the purpose of earthquake design [4]. Fiber-reinforced polymer, or FRP, has become a competitive substitute for conventional steel rebar in the strengthening of reinforced concrete structures. However, the malleability of FRP R.C. members is greatly reduced by the fragile nature of fiber-reinforced polymer. It is recommended that longitudinal reinforcement be added to the steel rebars to generate a hybrid reinforcement in order to improve the flexural ductility of FRP R.C. members [5]. When concrete infrastructure is exposed to hostile environments, like maritime environments and de-icing salts, it is very prone to corrosion. Fiber-reinforced polymer (FRP) reinforcements can be used in place of steel bars, as demonstrated by decades of intensive research. Compared to steel, fiber-reinforced polymer (FRP) reinforcements have a lower modulus of elasticity, a linear stress-strain relationship, superior strength-to-weight ratio, excellent fatigue resistance, and great corrosion resistance. Presently, glass, carbon, aramid, and basalt fibers are accessible for commercial use. These fibers are used to make GFRP, CFRP, AFRP, and BFRP rods, in that order. Because GFRP bars are relatively inexpensive, they are frequently utilized as reinforcement for concrete constructions rather than typical steel reinforcing bars [6]. Replace steel rebar at corners or on the outside of the tensile zone with FRP bars to reduce steel corrosion and increase the life of the hybrid RC beam [7, 8]. In order to confirm the torsional strength of the RC beam, Rahal [9] provided the findings of 66 beam tests. Relationships between torsional strength and concrete strength, as well as between torsional strength and the quantity of longitudinal and transverse reinforcement, have been noted.

*Corresponding Author.
E-mail address: alaa.alkhekany@qu.edu.iq ; Tel: (+964) 780-837 2180 (Alaa Al-Khekany)

https://doi.org/10.30772/qjes.2024.148224.1174

Nomenclature			
ACI	American Concrete Institute	*NSC*	Normal Strength Concrete
AFRP	Aramid Fiber- Reinforced Polymer	*NSM*	Near Surface Mounted
ASTM	American Society for Testing and Materials	*PPF*	Poly Propylene Fiber
BFRP	Basalt Fiber- Reinforced Polymer	*RC*	Reinforce Concrete
B.M	Bending Moment	*SCC*	Self-compacting concrete
CFRP	Carbon Fiber Reinforced Polymer	*SCRC*	Self-Compacting Reinforced Concrete
CB	Control Beam	*SF*	Steel Fiber
FRP	Fiber Reinforced Polymer	*SP*	Super Plasticizers
σ_u	Ultimate strength of steel	w/c	water-cement ratio
σ_y	Yield Stress of steel	Δh	Distance from the strengthened layer to the bottom of the control beam.
GFRP	Glass Fiber- Reinforced Polymer	Φ	Dimeter of reinforcement bar
Hpc	High-performance concrete	*Tu*	Ultimate torsion
IQS	The Iraqi Standards	ϕ	Angle of twist

Rahal also provided a straightforward technique for estimating the ultimate strength and mechanism of failure of reinforced concrete beams subjected to pure torsion. The findings demonstrated that ideas on the torsional behavior of longitudinal reinforcement and the concrete core area in reinforced concrete elements have been divergent for a considerable amount of time. While JM Gajipara et al. [10] studied the crack pattern in RC hollow beams subjected to cyclic torsion, the effect of core reinforcement and shear. Twelve beams were cast with unique combinations of longitudinal and shear reinforcement. Factors such as torque, torsion angle, energy dissipation, fracture mode, and failure mechanism were analyzed. The core reinforcement can withstand torsional moments after fracture, but is useless before cracking. The study highlights the importance of optimal spacing of transverse reinforcement in beam design. Regarding the study conducted by Patel et al. [11], where they examined the use of Glass Fiber Reinforced Polymer (GFRP) to improve torsional resistance in RC beams. The results showed significant increases in cracking, ultimate torque, and ultimate torsional deformations with different GFRP sheathing configurations. The study also found that diagonal strip sheathing was more effective than using vertical GFRP strips to resist torsional moment. Salamah presented, et al [12] studied the impact of seven beams' geometric parameters on the torsional strength of RC beams. The results showed that geometric factors such as flange width, flange height, and opening height had an impact on T-shaped RC beams under pure torsion. The behavior of RC beams subjected to joint buckling after being strengthened with U-shaped closed stirrups of NSM GFRP with varying overlap locations was examined by (Al-Zayadi and Al-Thiri) [13]. Four $150 \times 250 \times 2000mm$ reinforced concrete beams were examined; one was left unreinforced and used as a control beam (*CB*), while the other three were strengthened using different types of *NSM* and *GFRP* bars. *GFRP* closed stirrup beams with a 1000 *mm* rear overlap outperformed other reinforced beams by 181.5% as compared to the control beam CB. The 2000 *mm* U-shaped GFRP stirrups that reinforced the beam resulted in a torsional strength 48.1% lower than that of the *CB*. The usefulness of steel repair methods for fortifying reinforced concrete beams under torsional pressure was investigated by (Al-Zubaidi et al.) [14]. Six beams with the same diameters and spans were used in the study. The number of layers of reinforcing steel mesh and the composition of the ferrocement were the main subjects of the investigation. The findings indicate that the suggested methods have distinct impacts on the differently repaired beam's load capacity. Size has an impact on the torsional behavior of an *RC* beam with varying reinforcement ratios, according to research by M. Shokri et al. [15]. A statistical analysis was conducted on the torsional behavior of reinforced concrete beams that were either strengthened with *FRP* or not. Investigations were conducted on the torsional behavior of 24 specimens with varying section sizes and reinforcement ratios. Analyze and show the torque, end, and crushing torque curves. The findings showed that size had a considerable impact on the beams' torsional strength. Typically cracking the value rose from 1.72% to 36% when *FRP* textiles were used to reinforce the sill assembly. With a 0.4% increase in boost ratio, ultimate strength rose by 8.2%. The average cracking When the sill assemblies were reinforced with *FRP* textiles, the value increased by 1.72% to 36%. Ultimate strength increased by 8.2% with a boost ratio increased by 0.4%. NY ELWakkad et al. [16] ten self-compacting reinforced concrete beams reinforced with different external methods were tested mathematically and experimentally. Pure torsion is applied to GFRP laminates. Three layers of GFRP sheets along the specimen increased the ultimate torsional moment by 33.3%, the greatest increase. Four layers of GFRP laminates spaced every 300 *mm* increased the energy dissipation capacity by 209.4% compared to the non-reinforced sample. Furthermore, ABAQUS software performed a 3D nonlinear finite element analysis for the prediction. *GFRP* strips either reinforce the torsional properties of SCRC beams or leave them bare. The numerical model accurately reproduced the SCRC beams reinforced with the failure modes of the GFRP strips by comparing with the experimental results, torque versus twisting angle, stress distribution, and ultimate load. The torsional performance of high-performance rectangular reinforced concrete beams with polypropylene fiber (PPF) and steel fiber (SF) was compared by Karimipur et al. [17]. Under torsional stresses, nine beams reinforced with HPC were assessed. Additionally, SF and PPF at0,1,2, and 4% by volume were employed. Make use of the fiber beam as a guide. The torsional moment and torsion angle were both increased by PPF and SF, according to the experiments, with PPF-reinforced HPC beams exhibiting better torsional performance. More so than PPF, SF increased the HPC beam's torsional stiffness. The torsional moment strength rose by 122.3% and 85.2%, respectively, after the application of 4% PPF and SF, El-Mandouh et al. [18] The study used several strengthening methods to increase the torsional capacity of reinforced concrete beams. The research used six full-sized RC beams, a control beam, and six booster beams. The beam reinforced with stainless steel strips and laminated aluminum strips had 40% and 32% higher ultimate moments than the control beam. Although stainless steel strips cost more, these systems have increased productivity. The ultimate torque of GFRP-reinforced beams, single-layer laminated steel wire mesh, and double-layer laminated steel wire mesh is compared to control beams. Fully laminated steel wire mesh girders showed maximum ductility, while GFRP girders were least ductile (Alrawi MA et al.) [19]. The torsional behavior of near-surface steel-reinforced RC beams and CFRP bars was investigated. The results indicated good agreement in rotation torque, ultimate torque, rotation, and fracture pattern. ANSYS was used to examine thirteen specimens, the majority of which showed fractures at a stage 9% lower than the reference beam. The carbon rod replaced the rebar, boosting ultimate torsional strength by 3.5% while decreasing rotation by 4%. By reviewing and discussing the available research studies, it can be seen that very few studies have considered the effect of combined bending and torsion on the externally strengthened RC beams by enlargement section and hybrid reinforcement. The main objective of the current work is to study the combined bending and torsion behavior of externally strengthened RC beams by enlargement the section and hybrid reinforcement.

2. Experimental program

2.1 Beam specimens

Nine RC beams were used in this study; the cross-sectional dimensions were $150 \times 250mm$, a total length of 1750 *mm*, and a clear span of 1650 *mm*. They were subjected to two-point loads with an apparent distance of 550 *mm*, as shown in Fig. 1a. $3\phi12$ was used as longitudinal reinforcement in the tension region of the beam, and $2\phi10$ was used in the compression region as longitudinal reinforcement. Reinforcement of stirrups with a diameter of $\phi10mm$ at 100 *mm* center to center. The first stirrup is located at 75 *mm* from the face of the beam. Reference beam design according to the method in ACI 318-19 [20]. Fig. 1b shows the features of the beams after strengthening with Δh = 50 *mm* orΔh = 75 *mm* which shows the locations of steel (U) bars, shear connectors and details of hybrid reinforcement in the reinforcement layer.

2.2 Strengthening procedure

The study utilized the technique of enlarging the section by employing self-compacting concrete (SCC) in two groups as listed in Table 1. The first group had the thickness of the reinforcement layer 50 *mm* (Δh= 50 *mm*), and the second group had the thickness of the reinforcement layer 75 *mm* (Δh= 75 *mm*). This additional layer is reinforced with a different reinforcement between steel and reinforced polymer with fiberglass (GFRP) and hybrid bars (steel and GFRP). The following are the steps that illustrate the sample strengthening technique, Fig. 2.

- Create a U-shaped steel bar. The first group is 325 *mm* long and the

second group is 350 *mm* long. The steel bar was 10 *mm* wide and 3 *mm* thick.

- Put the measurements on the specimens by leaving a distance of 75mm from both sides. Then begin to determine the shear connector number 2 on the width of the beam, the distance between them, then move a distance of 100 *mm* and determine the first place for the steel bars(U) that hold the bars.
- Shear connectors are installed on the specimens, and steel bars (U) are bonded to the concrete using Sikadur-30LP (mix A and B) (a material used to bond steel to concrete).
- Wooden formwork (with 25 *mm* concrete cover provided) is installed at 75 *mm* (4 specimens) and 100 *mm* (4 specimens) from the original design, then reinforced. Models have different reinforcements.
- Begin installing the reinforcing bars for samples, as the reinforcement differs between steel, GFRP, and hybrid (GFRP Steel).
- After applying Sikadur-32LP, we poured the samples with new SCC concrete, a material used to bond old concrete to new concrete.
- Reinforced specimens have new cross-sectional dimensions. The first group (4 models) had a thickness of 50*mm*. Its dimensions were 150×325 *mm*, and the second group (4 models) had a thickness of 75 *mm*. Its dimensions are 150×350 *mm*.

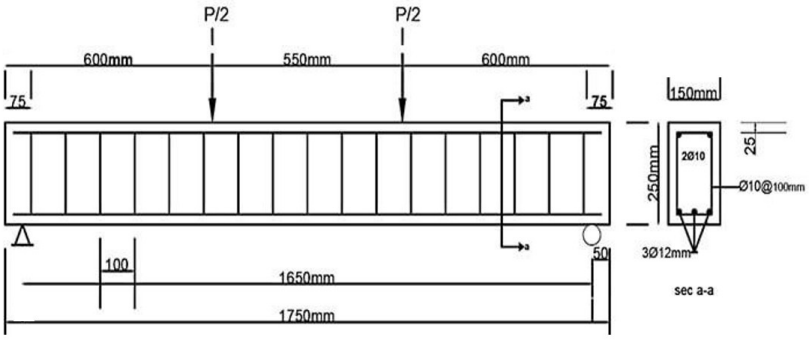

(a) Before strengthen

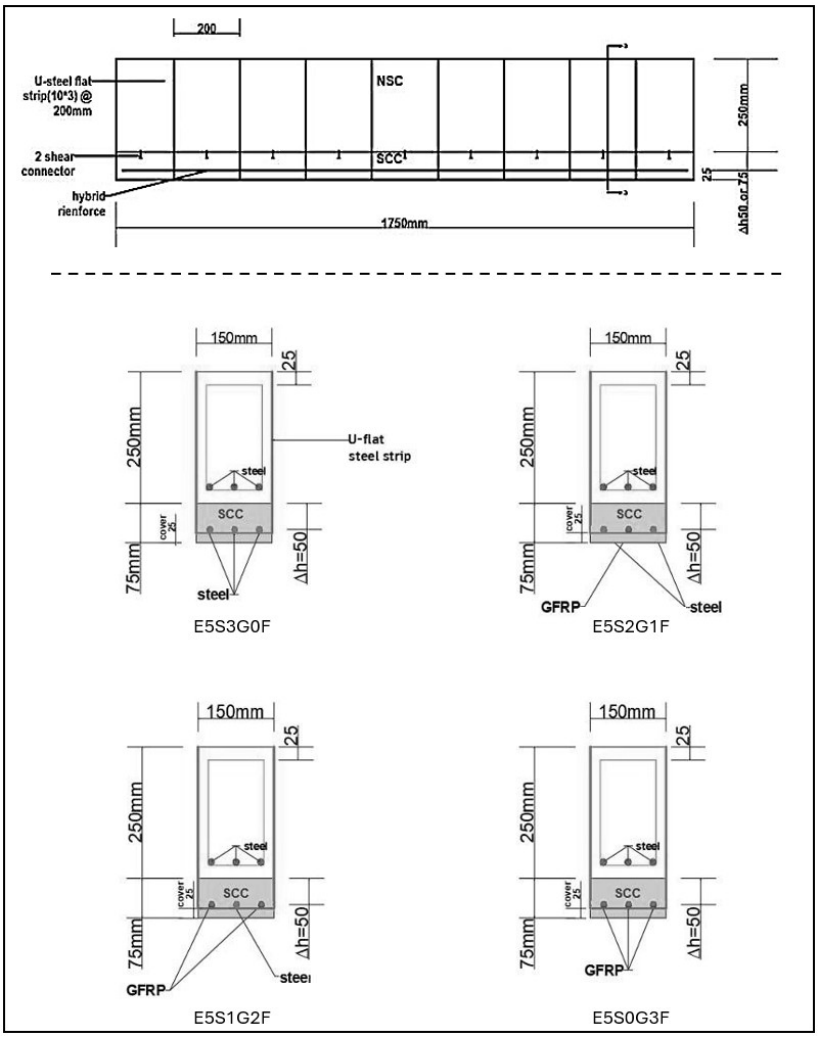

(b) After strengthen with Δh= 50*mm* or Δh= 75*mm* and hybrid reinforce

Figure 1. Details of reinforcement beams.

Table 1. Symbol of specimens.

RBC	Reference beam under combined
E5S3G0C	Enlargement of beam ($\Delta h = 50mm$) with 3 Steel and 0 GFRP Reinforcement under combined.
E5S2G1C	Enlargement of beam ($\Delta h = 50mm$) with 2 Steel and 1 GFRP Reinforcement under combined.
E5S1G2C	Enlargement of beam ($\Delta h = 50mm$) with 1 Steel and 2 GFRP Reinforcement under combined.
E5S0G3C	Enlargement of beam ($\Delta h = 50mm$) with 0 Steel and 3 GFRP Reinforcement under combined.
E7.5S3G0C	Enlargement of beam ($\Delta h = 75mm$) with 3 Steel and 0 GFRP Reinforcement under combined.
E7.5S2G1C	Enlargement of beam ($\Delta h = 75mm$) with 2 Steel and 1 GFRP Reinforcement under combined.
E7.5S1G2C	Enlargement of beam ($\Delta h = 75mm$) with 1 Steel and 2 GFRP Reinforcement under combined.
E7.5S0G3C	Enlargement of beam ($\Delta h = 75mm$) with 0 Steel and 3 GFRP Reinforcement under combined.

Table 2. Materials description.

Material	**Descriptions**
Cement	Portland Cement Ordinary (Type I) (IQS. No.5/1984) [21].
Fine aggregate (Sand)	Natural sand (zone 3) (IQS NO. 45/1984) [22].
Coarse aggregate (Gravel)	Coarse aggregate with a grading of (5-20) for Normal Strength Concrete (NSC) and (5-14) for Self-Compact Concrete (SCC)
Limestone powder	Limestone powder (LSP) (Al-Ghubra) is the marketing name for this material. The employed LP (less than 0.125 *mm*) complies with EFNARC standards for SCC [23].
Superplasticizer	Visco Crete-180 GS
Water	Conforming to the specifications for tap water.
GFRP Bar	The GFRP is the Russian type and has a diameter of 10 *mm*, σ_u for GFRP =827 *MPa*.
Steel Reinforcement Bars	Steel reinforcement Ukrainian sources were used in this research: $\phi 12$ for longitudinal reinforcement and $\phi 10$ for stirrups. ASTM associated with 615/A615M-09b [24]

2.3 Material properties

Table 2 lists the material's characteristics and descriptions that were used to make the specimens, and Table 3 lists the utilized steel details.

Table 3. Uniaxial tensile test results of steel reinforcing bars used in the present study.

Diameter (*mm*)	$\phi 10$	$\phi 12$	ASTM-615 Req.
Yield Stress σ_y (*MPa*)	552.02	547.30	420
Ultimate stress σ_u (*MPa*)	667.94	678.23	620

Table 4. Material composition of tested SCC concrete mixtures, kg/m^3.

Mix NO.	Cement	Sand	Gravel	LSP	Water	SP	w/c
1	430	750	825	145	187	3.4	0.43
2	480	720	820	135	181	3.8	0.38
3	490	725	830	128	178	4.0	0.36

Table 5. Test result of mix No3, which was chosen in this study.

Test	**Result**	**Range**
Slump flow(*mm*)	750	(650-800) *mm*
V-funnel (*sec.*)	8	(6 -12) *sec.*
L-box	1	(0.8.-1)

2.4 Concrete mix

•Normal Strength Concrete (NSC)

For normal-strength concrete (NSC), the required nominal compressive strength was 25 *MPa* for all specimens. The mixing ratio was 400, 800, 1100 cement, fine aggregate, and coarse aggregate respectively, with the water to cement ratio ($weight/g$) = 0.425.

•Self-Compacting Concrete (SCC)

Three mixing ratios for SCC mix [25,26] are listed in Table 4. To achieve SCC, make trial mixes by evaluating fresh concrete tests. According to EFNARC [27], SCC concrete production must pass ten different tests. In the present study, we used three tests, namely stagnant flow, L-box, and V-funnel, as control tests for the new SCC. Checking the ability to pass, fill criteria, and resist separation is essential. Table 5 shows the results of Mix No. 3 for SCC tests, which gives a compressive strength of approximately 37 *MPa*.

2.5 Casting and curing beam specimens

• First casting stage

The samples were cast and processed in the laboratory of the College of Engineering at Al-Qadisiyah University. The formwork was reinforced, and concrete was poured using central casting, three layers per formwork, with a steel rod used to level and polish the surface. After 24 hours, the wooden blocks were removed, and the model was misted with water for 28 days before being covered with a vacuum blanket.

• Second casting stage

The samples were processed and cast under laboratory conditions at 27°C. The reinforcement was placed inside steel (U) bars and cast using SCC concrete. The workers leveled and finished the concrete surface using a trowel. The formwork was removed after 24 hours, and the sills were treated for 28 days by spraying them with water and covering them with a vacuum blanket, as shown in Fig. 3.

3. Experimental test set-up

The experimental test set considered in this study can be divided into three components, namely: the RC beam specimens, the universal testing machine (test rig), and the measuring devices, including the load cell and the dial meter as shown in Fig. 5. All of the tests were carried out in the engineering college's laboratory at Al-Qadisiyah University. It was specifically intended to apply stress to beam specimens that will be assessed under torsion and bending using a loading frame with a 2000 *kN* capacity. As shown in Fig. 6, a certain support condition is made to permit rotation along the longitudinal axis, and lever arms are attached to the specimen to give a torsional moment. When the lever arm aligns with the support, the specimen is exposed to pure torsion. To apply combined torsion and bending, keep the lever arm distant from both supports. To apply different combinations of torsion and bending moment, the length and location of the lever arm can be changed. There are three dial gauges used: one in the center to measure central displacement, and two beneath the lever arm to measure displacements. To accomplish both bending and torsion, a 550 *mm* gap is kept between the lever arm and the center of support. The test setup's schematic design is displayed in Fig. 7. A spreader beam resting on the end of the lever arm transfers the weight of the hydraulic jack to the specimen. Each lever arm's end will therefore support half of the applied load. Coupled bending and torsion come from the load at the end of the lever arm being far from the specimen's support and the longitudinal axis of the beam. Adjusting the beam longitudinal axis with lever arms by 500 *mm*.

(a) Steel bar in the shape (U)

(b) Shear connector

(c) Drawing places for each shear

(d) Shear connector drill connector and steel bars (U)

(e) use Sikadur-30LP to install the Shear Connector and fixing steel bars (U).

(f) Installing the reinforcing bars

(g) Connecting the fresh concrete to the hardened concrete with sikadur-32LP

(h) Preparing the wooden mold to the second casting stage

Figure 2**.** Explain work-strengthening technique.

(a) Casting specimens

(b) Curing of specimens

Figure 3**.** The preparation steps of NSC Specimens.

(a) Casting specimens

(b) Curing of specimens

Figure 4**.** The reparation steps of SCC Specimens.

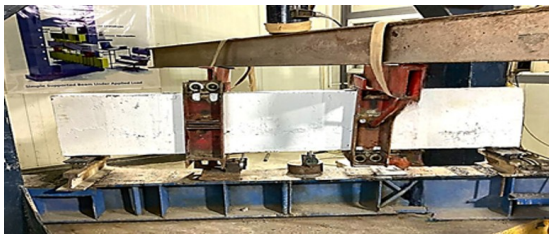

Figure 5**.** Test setup and loading frame used in this study.

Figure 6**.** The steel lever arms used to generate torsional moment.

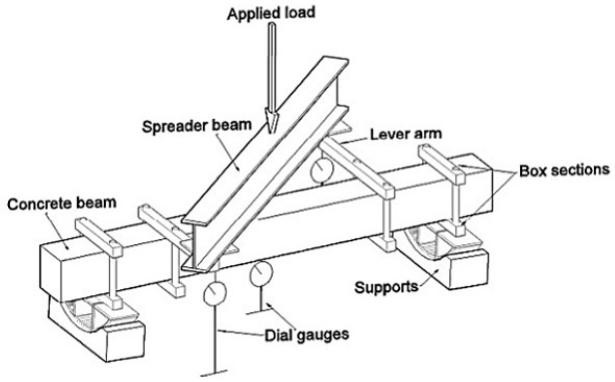

Figure 7**.** Schematic diagram of test set-up for applying combined torsion and bending [28].

Table 6**.** Summary of test results for tested specimens.

Group	Spe.	Pu (kN)	$B.M$ $(KN.m)$	Tu $(KN.m)$	$Tu/Tu_{(RBC)}$	$\phi_u{}^\circ$
Ref.	RBC	30	8.25	7.5	———	2.33
Group 1	E5S3G0C	50	13.75	12.50	66.67	3.89
	E5S2G1C	44	12.10	11.0	46.67	3.33
	E5S1G2C	43	11.82	10.75	43.33	3.11
	E5S0G3C	40	11.00	10.0	33.33	3.01
Group 2	E7.5S3G0C	60	16.50	15.0	100.0	5.53
	E7.5S2G1C	54	14.85	13.5	80.00	4.01
	E7.5S1G2C	50	13.75	12.5	66.67	3.55
	E7.5S0G3C	48	13.20	12.0	60.00	3.45

Where: $B.M = (P/2) \times (L/3)$ and L=1650 mm (Clear span)
And, $Tu = P/2 \times Arm$ and $Arm = 500mm$

4. Results and discussion

To better understanding the behavior of RC specimens-NCS and specimens-SCC by section expansion and hybrid reinforcement under combined torsion and bending is achieved, the specimens' development is monitored at regular intervals from torque until failure. The ultimate torque (Tu) is also measured in all samples. The failure mechanism of each specimen was studied to better understand the effect of section expansion reinforcement, hybrid reinforcement with steel, GFRP, and hybrid reinforcement (steel and GFRP) in torsional strengthening. The ultimate torsional moment (Tu) of beams reinforced using the section extension approach with thickness $\Delta h = 50mm$ rises by about (33.33%), (43.33%), (46.67%), and (66.67%) for beams E5S0G3C, E5S1G2C, E5S2G1C, and E5S3G0C as listed in Table 6. Compared to the

RC reference beam, the ultimate torsional moment (Tu) for the beams with thickness $\Delta h = 75mm$ rose by roughly (60%), (66.67%), (80%), and (100%) for the E7.5S0G3C beams, as well as E7.5S1G2C, E7.5S2G1C, and E7.5S3G0C respectively.

4.1 Control specimen (RB)

This specimen was cast without any strengthening techniques and was tested as a reference beam to compare behaviour with other strengthened specimens. The first crack appeared halfway along the sides at a load of 20 kN, with a twisting moment of about 5 $kN.m$ (33.3% of the ultimate twisting moment). As the loads increased, more diagonal cracks appeared on each side of the sill at different distances and spread upward. When the load reached the 30 4 torsion moment (7.5 $kN.m$), while the bending moment was (8.25 $kN.m$), failure occurred near the middle of the span at the torsion angle (2.33°). Figure 8 shows the crack pattern and failure mode of the specimen. Figure 9 shows the torque-angle of the twist curve for this specimen.

Figure 8. Failure mode and crack pattern of RB specimen.

4.2 Crack patterns and failure mode

4.2.1 First group

Figure 10 shows the cracking and failure modes of RC beams E5S3G0C and E7.5S3G0C, reinforced with three steel bars and 0 GFRP (this reinforcement is in the added reinforcement layer Δh =50 mm and Δh =75 mm). Beam E5S3G0C initiated the first diagonal crack at a load of 25 kN, with a twisting moment equal to 6.25 $kN.m$, while beam E7.5S3G0C showed the first diagonal crack at 46 kN with a twisting moment equal to 11.5 $kN.m$.

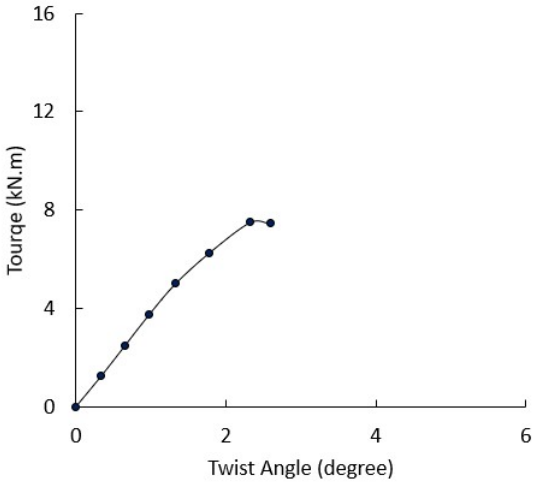

Figure 9. Torque-twist angle relationship of RB specimen.

The reason for this is that the section expansion in specimen E7.5S3G0C is greater compared to specimen E5S3G0C. For beam E5S3G0C, the appearance of diagonal cracks develops with increasing torsional torque applied to the beam until ultimate failure of the beam is reached. Load of 50 kN (ultimate torsional torque was 12.5 $kN.m$) and (ultimate bending moment was 13.75 $kN.m$).

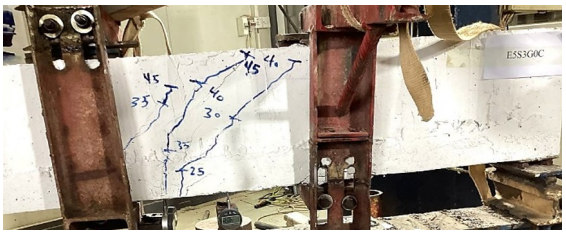

(a) E5S3G0C

(b) E7.5S3G0C

Figure 10. Shows the pattern of cracks.

Figure 10a shows that the final failure crack occurred at the top of the beam and was an obvious diagonal crack with a width of about 2 mm. As for beam E7.5S3G0C, diagonal torsional cracks appeared when the torsional moment was increased until the final torsional moment of 15 $kN.m$ was reached. It was the torque that caused the beam to fail. The presence of steel (U) bars in the sill as part of the reinforcement helped reduce the number of diagonal cracks in the sill. Adhesive bonding (Sikadur 30 LP) provides good bonding between steel bars and concrete. Therefore, until the final failure of both beams, we did not observe any pullout of the steel bars from the concrete. Epoxy bonding (Sikadur 32 LP) also provides good bonding between old and new concrete (NSC and SCC), as no separation occurs between the old and new concrete layers until the final failure of both beams.

(a) E5S0G3C

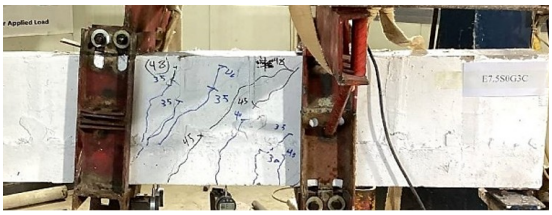

(b) E7.5S0G3C

Figure 11. Shows the pattern of cracks.

4.2.2 Second group

Figure 11 displays the beam failure types and crack patterns for E5S0G3C and E7.5S0G3C reinforced with three GFRP bars and 0 steel. E5S0G3C experienced the first diagonal crack at a load of 25 kN (with a twisting moment of 6.25 $kN.m$). While E7.5S0G3C witnessed the appearance of the first diagonal crack at a load of 30 kN (with a twisting torque equal to 7.5 $kN.m$), the E5S0G3C beam failed when the load reached 40 kN, with a twisting moment equal to 10 $kN.m$, and bending moment (11 $kN.m$) At this load, steel bars were pulled from the concrete. While specimen E7.5S0G3C failed at a load of 48 kN, at this load, steel bars were taken out of concrete. The reason for this difference in failure values between the two beams was due to the difference

in thickness of the section enlargement layer between them. No separation occurred between the old concrete and the new concrete (NSC and SCC) for both beams due to the use of shear connectors, as well as the use of epoxy (Sikadur 32LP), which strengthened the strength of the connection between the old concrete (NSC) and the new concrete (SCC).

(a) E5S2G1C

(b) E7.5S2G1C

Figure 12**.** Shows the pattern of cracks.

(a) E5S1G2C

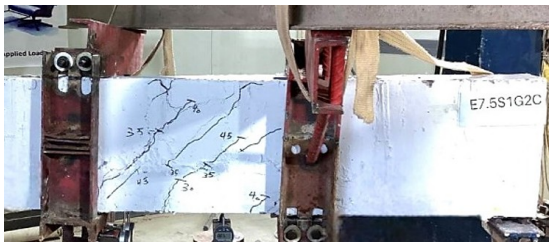

(b) E7.5S1G2C

Figure 13**.** Shows the pattern of cracks.

4.2.3 Third group

Figure 12 illustrates the beam failure types and crack patterns for E5S2G1C and E7.5S2G1C, reinforced with 2 steel and 1GFRP bars. E5S2G1C experienced its first diagonal torsional crack at 25 *kN* with a torsional torque of 6.25 *kN.m*., while beam E7.5S2G1C experienced its first diagonal torsional crack at a load of 30 *kN* with a torsional torque of 7.5 *kN.m*. The reason for the delayed onset of torsional crack at 30 kN load for beam E7.5S2G1C is the increased effective depth (section enlargement) compared to beam E5S2G1C. Steel bar removed from the concrete of beam E5S2G1C with a load of 44 *kN* (with a twisting moment of 11 *kN.m*.) and bending moment of 12.1 *kN.m*, which was also the ultimate failure moment for that beam. No steel bar was pulled out of the E7.5S2G1C beam, and radial torsion cracks continued to appear until the torsional moment reached 13.5 *kN.m*., the bending moment reached 14.85 *kN.m* the final moment of failure for that beam. No separation occurred between the old and new concrete layers, and this indicates the good bonding provided by both shear connectors and epoxy material between NSC and SCC.

4.2.4 Fourth group

Figure 13 shows the failure and fracture modes of beams E5S1G2C and E7.5S1G2C, strengthened with 1 steel and 2 GFRP bars. For both E5S1G2C and E7.5S1G2C, the first diagonal crack occurred at 30 *kN* (twisting moment equal to 7.5 *kNm*). The ultimate failure of beam E5S1G2C occurred at a load of 43 *kN* (with a torsional torque of 10.75 *kN.m*) and a bending moment of 11.82 *kN.m*, while failure of beam E7.5S1G2C occurred when the load reached 50 *kN* with torsion. The torque is 12.5 *kN.m*, and the bending torque is 13.75. The reason for this is the enlargement of the section. A force of 50 *kN* pulled the steel bar from the concrete of beam E7.5S1G2C. There was no separation between the two concrete layers due to good fixation using shear connectors and the epoxy used between the two layers of concrete.

4.3 Torque-angle of twist behaviour

4.3.1 First group

Figure 14 shows the torque angle curves of RC beams, which have the same reinforcement in the stiffening layer but different thicknesses. The control beam has a maximum torque of 7.5 *kN.m* and a rotation angle of 2.33°. Sample E5S3G0C has a maximum torque of 12.5 *kN.m* and a twist angle of 3.89°. This means that the E5S3G0C sample was 66.67% higher in torque than the control beam. While sample E7.5S3G0C has a maximum torque of 15 *kN.m* and a twist angle of 5.53°, this means that sample E7.5S3G0C had 100% and 20% higher torque than the control beam and sample E5S3G0C, respectively. The use of the beam section enlargement technique is due to the increase in the moment resistance and torsion angle of the beams supported by three steel bars when compared with the control beam and with each other.

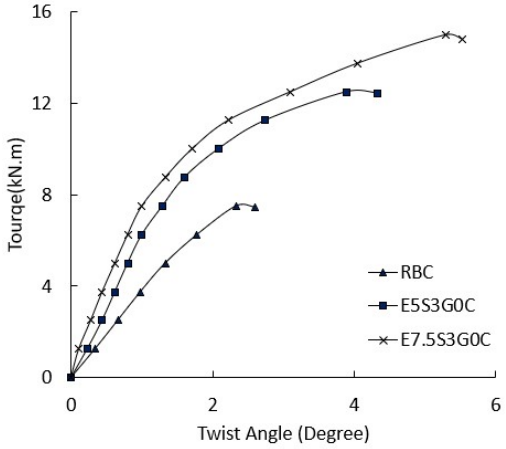

Figure 14**.** RC beam torque-angle twist curves strengthened with three steel bars.

4.3.2 Second group

Figure 15 shows the torque angle of torsion curves of reinforced RC beams having the same reinforcement layer but different thicknesses. The maximum torque of the reference beam is 7.5 *kN.m*, and the torsion angle is 2.33°, while the maximum torque of the E5S0G3C specimen is 10 *kN.m* and the torsion angle is 3.01°. Sample E7.5S0G3C has a maximum torque of 12 *kN.m* and a twist angle of 3.45°; Sample E5S0G3C was 33.33% higher in torque than the control beam. While the torque of E7.5S0G3C was 60% and 20% higher than control beam and E5S0G3C, respectively. The reason for the increased torque resistance and the increased torsion angle of the beams reinforced with three GFRP bars, when compared with the control beam and with each other, was due to the use of the beam section enlargement technique.

4.3.3 Third group

Figure 16 shows the torque–twist angle curves of reinforced RC beams that have the same reinforcement layer but different thicknesses, and hybrid reinforced bars (two steel and one GFRP) of E5S2G1C and E7.5S2G1C. The reference beam has a highest torque of 7.5 *kN.m* and a torsion angle of 2.33°, while the E5S2G1C sample has a maximum torque of 11 *kN.m* and a torsion angle of 3.33°. Sample E7.5S2G1C has a maximum torque of 13.5 *kN.m* and a twist angle of 4.01°; Sample E5S2G1C is 46.67% higher in torque than the control beam. While sample E7.5S2G1C is 80% and 22.7% higher in torque than the control beam and sample E5S2G1C, respectively, an increase in the effective depth resulted in increased tolerance of the reinforced beams

to torsional moments and an increased rotation angle when comparing the reinforced beams with the reference sample.

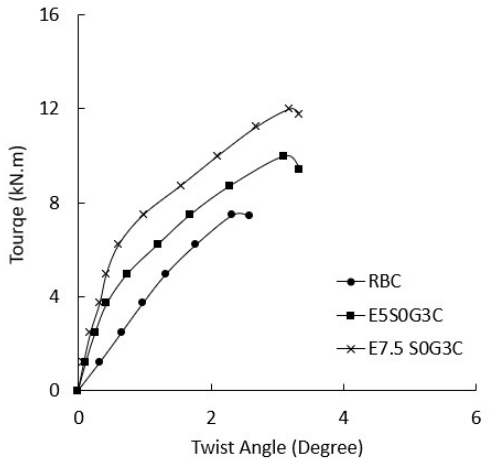

Figure 15**.** RC beam torque-angle twist curves strengthened with three GFRP bars.

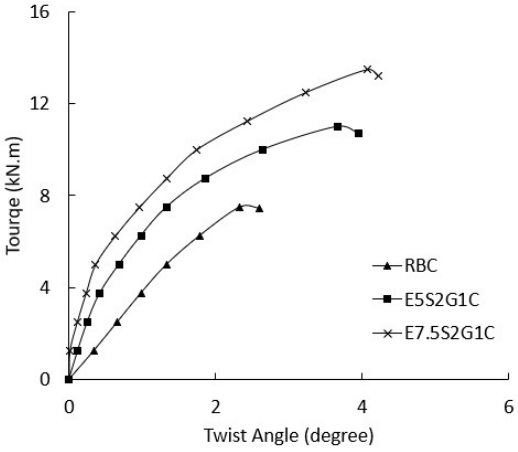

Figure 16**.** RC beam torque-angle twist curves strengthened with hybrid reinforcement.

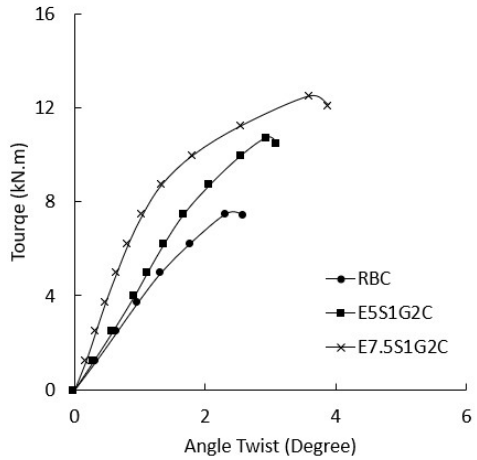

Figure 17**.** RC beam torque-angle twist curves strengthened with hybrid reinforcement.

4.3.4 Fourth group

Figure 17 shows the torque–twist angle curves of reinforced RC beams that have the same reinforcement in the additional layer but different thicknesses, and hybrid reinforced bars (one steel and two GFRP) of E5S1G2C and E7.5S1G2C bars. The reference beam has a maximum torque of 7.5 *kN.m.* and a torsion angle of 2.33°, while the E5S1G2C sample has a maximum torque of 10.75 *kN.m.* and a torsion angle of 3.11°. Specimen E7.5S1G2C has a maximum torque of 12.5 *kN.m.* and a twist angle of 3.55°. Specimen E5S1G2C is 43.33% higher in torque than the control beam, and the torsion angle of this beam is 33.5% higher than the control beam angle twist. While specimen E7.5S1G2C is 66.67% and 16.3% higher in torque than the control beam and sample E5S1G2C, respectively, the torsion angle of this beam is 52.4% and 14.15% above the control beam and sample E5S1G2C. The use of hybrid bars is a notable feature in the reinforcement layer (one steel and two GFRP). Increasing the effective depth resulted in increased tolerance to torsional moments and an increased rotation angle when comparing the reinforced beams with the reference sample.

4.4 Effect of reinforcement replacement with $\Delta h = 50mm$

The torque angle curves of the reference beam, the RC beams E5S3G0C, E5S2G1C, E5S1G2C, and E5S0G3C are shown in Figure 18. These beams all have the same section expansion layer (Δh = 50 *mm*) and different types of reinforcement, such as steel, GFRP, and a hybrid type of reinforcement (steel and GFRP). The E5S3G0C specimen has a maximum torque of 12.5 *kN.m*, which is 66.67% greater than the reference beam RB. The E5S2G1C specimen has a maximum torque of 11 *kN.m*, which is higher than the reference beam but lower than the E5S3G0C. The E5S1G2C specimen's maximum torque is 10.75 *kN.m*, which is 43.33% higher than the reference beam but lower than the E5S2G1C beam. The E5S0G3C sample has a maximum torque of 10 *kN.m*, which is 33.33% higher than the reference beam but 6.97%, 9%, and 20% lower than that of the E5S1G2C, E5S2G1C, and E5S3G0C, respectively. It was found that the beam E5S3G0C (reinforced with 3 steel bars in the enlarged section) recorded the highest torque among the other beams. The specimen E5S0G3C, which was reinforced with 3 GFRP in the expanded section, had the lowest torsional torque of all the samples. This was because using GFRP alone as reinforcement in the section expansion layer has a number of problems, such as brittle failure and a low modulus of elasticity, which means it has less torsional resistance.

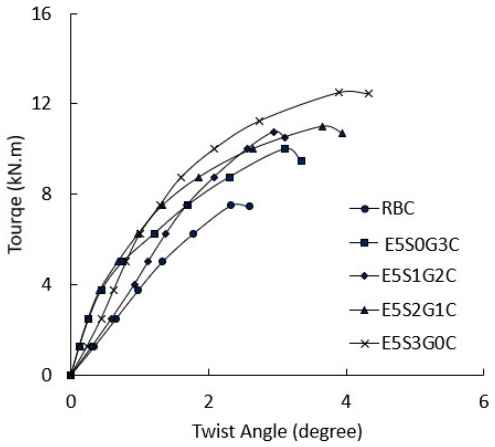

Figure 18**.** RC beam torque-angle twist for control and strengthened beams with Δh = 50 *mm*.

4.5 Effect of reinforcement replacement with $\Delta h = 75mm$

Figure 19 displays the torque angle curves of the reference beam, the RC beams E7.5S3G0C, E7.5S2G1C, E7.5S1G2C, and E7.5S0G3C. These beams all have the same section expansion layer ($\Delta h = 75mm$) and different types of reinforcement, such as steel, GFRP, and a hybrid type of reinforcement (steel and GFRP). The E7.5S3G0C specimen has a maximum torque of 15 *kN.m*, which is 100% higher than the control beam, and a maximum twist angle of 5.53°. The E7.5S2G1C beam has a maximum torque of 13.5 *kN.m*, which is 80% higher than the control beam and 10% lower than the E7.5S3G0C beam. The maximum torque of the E7.5S1G2C sample is 12.5 *kN.m*, which is 66.67% higher than the control beam and 16.67% lower than the E7.5S3G0C. The E7.5S0G3C sample has a maximum torque of 12 *kN.m*, 60% greater than the control beam. GFRP-reinforced beams have a lower twisting moment, causing

more deformation compared to RC steel beams. It was found that the beam E7.5S3G0C (reinforced with 3 steel bars in the enlarged section) recorded the highest torque among the other beams. The specimen E7.5S0G3C, reinforced with 3 GFRP in the expanded section, exhibited the lowest torsional torque among all the samples. This is because using GFRP alone as reinforcement in the section expansion layer has a number of problems, such as brittle failure and a low modulus of elasticity, which means it has less torsional resistance.

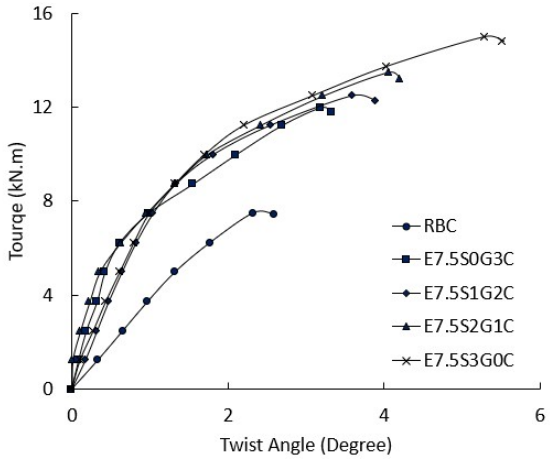

Figure 19**.** RC beam torque-angle twist for control and strengthened beams with Δh = 75 *mm*.

5. Conclusions

This work presents experimental research conducted under combined bending and torsion conditions on steel-reinforced RC beams, GFRP, hybrid reinforced bars, and section enlargement technologies. Experiments were conducted on nine RC beams. While the other eight specimens were strengthened using steel-GFRP, hybrid reinforcement (steel and GFRP), and section enlargement procedures, one of them served as a control beam. Every beam specimen was put under torsional strain until it broke. The investigation looked at torque angle curves, failure loads and moments, crack patterns, and failure mechanisms. The primary findings from the experiment are presented in the section that follows:

- Reinforcing RC beams with steel, GFRP, and hybrid bars (steel and GFRP) improves the beam's ability to withstand combined bending and torsional moments. A study using steel bars showed that increasing the effective depth by 50 *mm* and 75 *mm* resulted in the largest increase in the beam tolerance to ultimate torsional moment, which was approximately 66.67% and 100% of the control beam, respectively.
- The use of hybrid relays:
  In RC beams resulted in torsional capacity enhancement of 46.67% and 80% using steel bars and GFRP with effective depth Δh = 50 *mm* and Δh = 75 *mm*, respectively. The reason was the increased effective depth of Δh = 50 *mm* and Δh = 75 *mm*.
  Reinforcing the RC beams with one steel and two GFRP bars improved the ultimate torsional capacity by 43.33% and 66.67% of the control beam, as a result of the effective depth increased by Δh = 50 *mm* and Δh = 75 *mm*.
  Reinforcing RC beams with three GFRP bars improved the ultimate torsional capacity by 33.33% and 60% of the control beam, due to the increase in effective depth by Δh = 50 *mm* and Δh = 75 *mm*.
- Adhesive (Sikadur-30LP) stabilizes the steel bars (U) that secure the reinforcement to concrete and can reduce the appearance of radial torsion cracks in the specimen.
- RC tests revealed significant improvements in maximum torsional capacity:
  Compared to the control sample, when increasing the effective depth Δh=50 *mm*, it led to an increase in the final torsional capacity from 33.33% to 66.67%.
  When increasing the effective depth Δh=75 *mm*, it led to an increase in the maximum torsional strength of the reinforced beams from 60% to 100% compared to the control sample.
- The purpose of fixing the shear connector on the surface of the specimens and using an adhesive (Sikadur-32LP) to attach the old layer of Normal Strength Concrete (NSC) to the new layer of self-compacting concrete (SCC) is to prevent a longitudinal crack separating the two layers when used in most specimens.
- The proposed method for strengthening RC beams under combined bending and torsion improved the overall results and is reliable for strengthening structural elements.

Authors' contribution

All authors contributed equally to the preparation of this article.

Declaration of competing interest

The authors declare no conflicts of interest.

Funding source

This study didn't receive any specific funds.

Data availability

The data that support the findings of this study are available from the corresponding author upon reasonable request.

REFERENCES

[1] V. Jariwala, P. Patel, and S. Purohit, "Strengthening of rc beams subjected to combined torsion and bending with gfrp composites," *Procedia Engineering*, vol. 51, pp. 282–289, 2013. [Online]. Available: https://doi.org/10.1016/j.proeng.2013.01.038

[2] R. Park and T. Paulay, *Reinforced Concrete Structures*. John Wiley Sons, Ltd, 1975, pp. i–xvii. [Online]. Available: https://doi.org/10.1002/9780470172834.fmatter

[3] A. Aziz and O. Hashim, "Torsional strength evaluation of reinforced scc box beams strengthened internally by opened and closed transverse concrete diaphragms," *MATEC Web Conf.*, vol. 162, no. 04009, p. 9, 2018. [Online]. Available: https://doi.org/10.1051/matecconf/201816204009

[4] H. Naderpour, O. Poursaeidi, and M. Ahmadi, "Shear resistance prediction of concrete beams reinforced by frp bars using artificial neural networks," *Measurement*, vol. 126, pp. 299–308, 2018. [Online]. Available: https://doi.org/10.1016/j.measurement.2018.05.051

[5] L. S. Al-Yassri, A. Y. Ali, and M. M. AL-Khafaji, "Experimental investigation for the behavior of hollow core concrete slab reinforced with hybrid reinforcement," *Al-Qadisiyah Journal for Engineering Sciences*, vol. 10, no. 3, pp. 308–317, 2017. [Online]. Available: https://qjes.qu.edu.iq/article_131619.html

[6] W. Xue, F. Peng, and Q. Zheng, "Design equations for flexural capacity of concrete beams reinforced with glass fiber–reinforced polymer bars," *Journal of Composites for Construction*, vol. 20, no. 3, p. 04015069, 2016. [Online]. Available: https://doi.org/10.1061/(ASCE)CC.1943-5614.0000630

[7] W. Qu, X. Zhang, and H. Huang, "Flexural behavior of concrete beams reinforced with hybrid (gfrp and steel) bars," *Journal of Composites for construction*, vol. 13, no. 5, pp. 350–359, 2009. [Online]. Available: https://doi.org/10.1061/(ASCE)CC.1943-5614.0000035

[8] A. Acciai, A. D'Ambrisi, M. De Stefano, F. F. Feo, L., and R. Nudo, "Experimental response of frp reinforced members without transverse reinforcement: Failure modes and design issues," *Composites Part B: Engineering*, vol. 89, pp. 397–407, 2016. [Online]. Available: https://doi.org/10.1016/j.compositesb.2016.01.002

[9] K. N. Rahal, "Torsional strength of reinforced concrete beams," *Canadian Journal of Civil Engineering*, vol. 27, no. 3, pp. 445–453, 2000. [Online]. Available: https://doi.org/10.1139/l99-083

[10] J. M. Gajipara, P. V. Patel, and S. D. Raiyani, "Behavior of rc hollow beam under pure cyclic torsion," *Int J Res in Eng. Technol.*, vol. 04, no. 13, pp. 407–412, 2015. [Online]. Available: https://ijret.org/volumes/2015v04/i25/IJRET20150425060.pdf

[11] S. B. Tibhe and V. R. Rathi, "Comparative experimental study on torsional behavior of rc beam using cfrp and gfrp fabric wrapping," *Procedia Technology*, vol. 24, pp. 140–147, 2016. [Online]. Available: https://doi.org/10.1016/j.protcy.2016.05.020

[12] A. E. Salama, M. E. Kassem, and A. A. Mahmoud, "Torsional behavior of t-shaped reinforced concrete beams with large web openings," *Journal of Building Engineering*, vol. 18, pp. 84–94, 2018. [Online]. Available: https://doi.org/10.1016/j.jobe.2018.02.004

[13] A. C. Al-Ziady and H. Al-Thairy, "Torsional behaviour of rc beams strengthened by nsm gfrp bars," *In IOP Conference Series: Earth and Environmental Science*, vol. 1232, no. 1, p. 012037, 2023. [Online]. Available: https://doi.org/10.1088/1755-1315/1232/1/012037

[14] S. Alzabidi, G. Diaa, A. Abadel, K. Sennah, and H. Abdalla, "Rehabilitation of reinforced concrete beams subjected to torsional load using ferrocement," *Case Studies in Construction Materials*, vol. 19, no. 4, p. e02433, 2023. [Online]. Available: https://doi.org/10.1016/j.cscm.2023.e02433

[15] A. Committee, "318-19 building code requirements for structural concrete and commentary," *ACI*, 2019. [Online]. Available: https://api.semanticscholar.org/CorpusID:243163499

[16] M. Shokri, M. Edalati, S. Mirhosseini, and E. Zeighami, "Fe analysis on size effect in torsional behavior of rectangular rc beams with and without frp strengthening," *KSCE Journal of Civil Engineering*, vol. 28, no. 5, pp. 1836–1852, 2024. [Online]. Available: https://doi.org/10.1007/s12205-024-0020-0

[17] N. ELWakkad, K. Heiza, and W. Mansour, "Experimental study and finite element modelling of the torsional behavior of self-compacting reinforced concrete (scrc) beams strengthened by gfrp," *Case Studies in Construction Materials*, vol. 18, p. e02123, 2023. [Online]. Available: https://doi.org/10.1016/j.cscm.2023.e02123

[18] A. Karimipour, J. De Brito, M. Ghalehnovi, and O. Gencel, "Torsional behaviour of rectangular high-performance fibre-reinforced concrete beams," *Structures*, vol. 35, pp. 511–519, 2022. [Online]. Available: https://doi.org/10.1016/j.istruc.2021.11.037

[19] M. El-Mandouh, J. Hu, W. Shim, F. Abdelazeem, and G. ELsamak, "Torsional improvement of rc beams using various strengthening systems," *Buildings*, vol. 12, no. 11, p. 1776, 2022. [Online]. Available: https://doi.org/10.3390/buildings12111776

[20] A. MA and M. MN., "Strengthening reinforced beams subjected to pure torsion by near surface mounted rebars," *Anbar Journal for Engineering Sciences.*, vol. 13, no. 1, pp. 13–22, 2022. [Online]. Available: https://doi.org/10.37649/aengs.2022.175876

[21] "Iraqi standard specification (iqs) no.5.for portland cement central organization for standardization and quality," 2019. [Online]. Available: https://iraqi-standards.org/Home/Ssection

[22] "Iraq standard specification (iqs) no.45 natural sources of aggregate used in building and concrete, baghdad, 13p." 2019. [Online]. Available: https://iraqi-standards.org/Home/Ssection

[23] Group, "The european guidelines for self compacting concrete represent a state-of-the-art document addressed to specifiers, designers, purchasers, producers and users who wish to enhance their expertise and use of scc," *European Guidelines for Self Compacting Concrete (SCC)*, 2005. [Online]. Available: www.efnarc.org

[24] ASTM-A615/A615M-09b, "Standard specification for deformed and plain carbon-steel bars for concrete reinforcement," 2009. [Online]. Available: https://doi.org/10.1520/A0615_A0615M-09B

[25] M. S. Abo Dhaheer, M. M. Al-Rubaye, W. S. Alyhya, B. L. Karihaloo, and S. Kulasegaram, "Proportioning of self–compacting concrete mixes based on target plastic viscosity and compressive strength: part i-mix design procedure." *Journal of Sustainable Cement-Based Materials*, vol. 5, no. 4, pp. 199–216, 2016. [Online]. Available: https://doi.org/10.1080/21650373.2015.1039625

[26] W. S. e. a. Alyhya, "A rational method for the design of self-compacting concrete mixes based on target plastic viscosity and compressive strength," *Aberdeen, UK,35th Cement concrete science conference (CCSC35*, p. 85–9, 2015. [Online]. Available: https://doi.org/10.1088/1757-899X/671/1/012117

[27] M. Solikin, Basuki, and B. Setiawan, "The utilization of self compacting concrete (scc) in producing hollow concrete panel wall to provide rapid shelter for post disaster area," *Procedia Engineering*, vol. 54, pp. 742–751, 2013, the 2nd International Conference on Rehabilitation and Maintenance in Civil Engineering (ICRMCE). [Online]. Available: https://doi.org/10.1016/j.proeng.2013.03.068

[28] V. H. Jariwala, P. V. Patel, and S. P. Purohit, "Strengthening of rc beams subjected to combined torsion and bending with gfrp composites," *Procedia Engineering*, vol. 51, pp. 282–289, 2013, chemical, Civil and Mechanical Engineering Tracks of 3rd Nirma University International Conference on Engineering (NUiCONE2012). [Online]. Available: https://doi.org/10.1016/j.proeng.2013.01.038

How to cite this article:
Abrar R. Al-Rammahi, Alaa M. Al-Khekany, and Gy¨orgy L. Bal´azs. (2025). 'Combined bending and torsion behavior of externally strengthened RC beams via enlargement section and hybrid reinforcement', Al-Qadisiyah Journal for Engineering Sciences, 18(4), pp. 465-474. https://doi.org/10.30772/qjes.2024.148224.1174